arXiv:0707.3429v1 [astro-ph] 23 Jul 2007

THE HOT INNER DISK OF FU ORI

Zhaohuan Zhu[1], Lee Hartmann[1], Nuria Calvet[1],Jesus Hernandez[1,3], James Muzerolle[2],
Ajay-Kumar Tannirkulam[1]

ABSTRACT

We have constructed a detailed radiative transfer disk model which reproduces the main features of the spectrum of the outbursting young stellar object FU Orionis from ~ 4000 Å to $\sim 8\mu$m. Using an estimated visual extinction $A_V \sim 1.5$, a steady disk model with a central star mass $\sim 0.3 M_\odot$ and a mass accretion rate $\sim 2\times10^{-4} M_\odot \mathrm{yr}^{-1}$, we can reproduce the spectral energy distribution of FU Ori quite well. Higher values of extinction used in previous analysis ($A_V\sim$ 2.1) result in spectral energy distributions which are less well-fitted by a steady disk model, but might be explained by extra energy dissipation of the boundary layer in the inner disk. With the mid-infrared spectrum obtained by the Infrared Spectrograph (IRS) on board the *Spitzer Space Telescope*, we estimate that the outer radius of the hot, rapidly accreting inner disk is ~ 1 AU using disk models truncated at this outer radius. Inclusion of radiation from a cooler irradiated outer disk might reduce the outer limit of the hot inner disk to ~ 0.5 AU. In either case, the radius is inconsistent with a pure thermal instability model for the outburst. Our radiative transfer model implies that the central disk temperature $T_c \geq 1000$ K out to $\sim 0.5 - 1$ AU, suggesting that the magnetorotational instability can be supported out to that distance. Assuming that the ~ 100 yr decay timescale in brightness of FU Ori represents the viscous timescale of the hot inner disk, we estimate the viscosity parameter to be $\alpha \sim 0.2 - 0.02$ in the outburst state, consistent with numerical simulations of the magnetorotational instability in disks. The radial extent of the high $\dot{M}$ region is inconsistent with the model of Bell & Lin, but may be consistent with theories incorporating both gravitational and magnetorotational instabilities.

---

[1] Dept. of Astronomy, University of Michigan, 500 Church Street, Ann Arbor, MI 48109;zhuzh@umich.edu,lhartm@umich.edu,ncalvet@umich.edu,hernandj@umich.edu,hernandj@umich.edu

[2] Steward Observatory, 933 North Cherry Avenue, University of Arizona,Tucson, AZ 85721;jamesm@as.arizona.edu

[3] Centro de Investigaciones de Astronomia, Apartado Postal 264, Merida 5101-A, Venezuela

Subject headings: accretion disks, circumstellar matter, stars: formation, stars: pre-main sequence

1. Introduction

The FU Orionis systems are a small but remarkable class of variable young objects which undergo outbursts in optical light of 5 magnitudes or more (Herbig 1977), with a F-G supergiant optical spectra and K-M supergiant near-infrared spectra dominated by deep CO overtone absorption. While the rise times for outbursts are usually very short ($\sim$ 1-10 yr), the decay timescales range from decades to centuries. The FU Ori objects also show distinctive reflection nebulae, large infrared excesses of radiation, wavelength dependent spectral types, and "double-peaked" absorption line profiles (Hartmann & Kenyon 1996). The frequency of these outbursts is uncertain; in recent years an increasing number of heavily extincted potential FU Ori objects have been identified on the basis of their spectroscopic characteristics at near-infrared wavelengths (Kenyon et al. 1993; Reipurth & Aspin 1997; Sandell & Aspin 1998; Aspin & Reipurth 2003).

The accretion disk model for FU Ori objects proposed by Hartmann & Kenyon (1985, 1987a, 1987b) and Kenyon et al. (1988) can explain the peculiarities enumerated above in a straightforward manner. Outbursts are known in other accreting disk systems and may be the result of a common mechanism (e.g., Bell & Lin 1994). The high temperature of the inner disk produces the observed F-G supergiant optical spectrum, while the cooler outer disk produces an infrared spectrum having the spectral type of a K-M supergiant. The Keplerian rotation of the disk can produce double-peaked line profiles as often observed, with peak separation decreasing with increasing wavelength of observations, since the inner hotter disk which produces the optical spectrum rotates faster than the outer cooler disk which produces the infrared spectrum (Hartmann & Kenyon 1996).

While the accretion disk model has been successful so far, it is important to continue to test it and to derive further insights into the origins of the accretion outbursts as new observations become available. In particular, the mid-infrared spectrum obtained with the Infrared Spectrograph (IRS) on the *Spitzer Space Telescope* provides important constraints on the outer edge of the hot inner disk (Green et al. 2006), which in turn can test theories of outbursts. For example, the thermal instability model of Bell & Lin (1994) predicts an outer radius for the outburst region of only $\sim 20\mathrm{R}_\odot$, which is smaller than that estimated by Green et al. (2006) on the basis of simple blackbody disk models. Armitage et al. (2001) suggested that a combination of gravitational instability (GI) with triggering of the magnetorotational instability (MRI) might also explain FU Ori outbursts; in this model the high accretion rate region in outburst would be much larger, of order 0.5 AU. Vorobyov & Basu (2005,2006) suggested that FU Ori outbursts could also be produced by the accretion of clumps formed in a gravitationally unstable disk. This model predicts high accretion rates at its inner radius of 10 AU. These differing predictions for the size of the outburst region should be testable with detailed models of the spectral energy distribution (SED). Furthermore, if we can constrain the size of the outburst region, the timescales of decay may provide quantitative estimates of the viscosity, vital for understanding the evolution of young protoplanetary disks.

In this paper we present new steady, optically-thick accretion disk spectrum calculations, and compare the results with observations from the ultraviolet to the mid-infrared of FU Ori−the prototype of these systems. In §2 we describe the observational material used to constrain the models, while in §3 we describe the methods used to calculate the disk models. We show in §4 that the steady disk model reproduces the variation of the observed spectral features over this very large wavelength range quite well. In §5 we consider some implications of our results for disk viscosities, outburst mechanisms, and disk masses, and summarize our conclusions in §6.

2. Optical and infrared data

An essential part of the spectral energy distribution (SED) of FU Ori for our model is the IRS spectrum from *Spitzer* observed on March 4, 2004 (see Green et al. 2006 for details). As FU Ori has been fading slowly over the last 60 years, we need to obtain data at other wavelengths near the same time as the IRS spectrum to construct a complete spectral energy distribution (SED).

Optical photometry (UBVR) was obtained in 2004 at the Maidanak Observatory (Ibrahimov 1999; Green et al. 2006). As FU Ori exhibits small, irregular variability on timescales much less than a year, we averaged the Maidanak data to form the mean values (with RMS uncertainty in each band ∼ 0.02 magnitude) used in this paper. In addition, we include an optical spectrum of FU Ori obtained on March 27th, 2004, near the time of the IRS observations, using the 1.5m telescope of the Whipple Observatory with the FAST Spectrograph (Fabricant et al. 1998), equipped with the Loral 512 × 2688 CCD. This instrument provides 3400 Å of spectral coverage centered at 5500 Å, with a resolution of 6 Å. The spectrum was wavelength calibrated and combined using standard IRAF routines [1]. The spectrum was corrected for the relative system response using the IRAF *sensfunc* task. The optical spectrum was placed on an absolute flux scale using the averaged 2004 UBVR photometry.

---

[1] IRAF is distributed by the National Optical Astronomy Observatories, which are operated by the Association of Universities for Research in Astronomy, Inc., under cooperative agreement with the National

Near-infrared fluxes were determined from several sources. 2MASS JHK photometry is available from October 7th, 1999, five years before IRS observations. We also include data from Reipurth & Aspin (2004) on December 15, 2003, using the NAOJ 8 m Subaru Telescope on Mauna Kea and the Infrared Camera and Spectrograph (IRCS). Finally, we obtained JHK magnitudes on December 17th 2005, using the Near-IR Imager/Spectrometer TIFKAM on the 2.4 m MDM telescope at Kitt Peak. Although the 2.4m telescope had to be defocused to avoid saturation because FU Ori is so bright, our JHK magnitudes of 6.57, 5.91 and 5.33, respectively, are in reasonable agreement with the JHK$_s$ 2MASS magnitudes of 6.519, 5.699, 5.159, respectively, indicating that the FU Ori fluxes have not changed dramatically over that six year period. The Reipurth & Aspin (2004) observations are on a different system, but when converted to fluxes yield reasonably similar results. We therefore adopted the 2MASS magnitudes as our standard in this wavelength region.

We then incorporated the KSPEC spectrum (resolution R$\sim$500, 1.15-2.42μm) observed on Dec 15th, 1994 by Greene & Lada (1996) and the observation with SpeX (2.1-4.8μm) on the Infrared Telescope Facility (IRTF; Rayner et al. 1998) obtained during the nights of January 5-6th, 2001 (see Muzerolle et al. 2003 for details). We placed these spectra on an absolute scale by convolving the spectra with the relative spectral response curve (RSRs) of the 2MASS system (Cohen et al. 2003) and tying the overall result to the 2MASS K$_s$ magnitude.

The collected observations are shown in Figure 1, where we assume an A$_V$ of 1.5 instead of the usually assumed value of $\sim$ 2.2 (Kenyon et al. 1988; KHH88). The previously discussed variation of spectral type with wavelength is immediately apparent in Figure 1; the optical spectrum corresponds to a G type spectrum as estimated from the atomic metal lines while the near-IR and IRS wavelength ranges are dominated by molecular bands indicative of a much later spectral type. While the optical and infrared spectra are dominated by absorption features, dust emission dominates longward of 8 μm, as shown by the silicate emission features at 10 and 20 μm.

Science Foundation.

3. Model

In this paper we only model the absorption spectrum (λ<8 μm) which is produced by the centrally-heated accretion disk. The silicate emission features are produced by externally-heated regions of the outer disk or possibly a circumstellar dusty envelope (Kenyon & Hartmann 1991; Green et al. 2006); we defer modeling of this region to a subsequent paper.

We follow the method of Calvet et al. (1991a,b) to calculate the disk spectrum. In summary, we calculate the emission from the atmosphere of a viscous, geometrically thin, optically thick accretion disk with constant mass accretion rate $\dot{M}$ around a star with mass M and radius R. The disk height H is assumed to vary with the distance from the rotational axis of the star R as $H = H_0(R/R_i)^{9/8}$, where we take $H_0 = 0.1R_i$ and R_i is the radius of the central star. This approximation is not very accurate but it only affects the local surface gravity of the disk atmosphere, which has only a small effect on the emergent spectrum. Viscous dissipation in the atmosphere is neglected, which is a good approximation for cases of interest (Hartmann & Kenyon 1991). Thus, radiative equilibrium holds in the disk atmosphere, and the surface flux is determined by the viscous energy generation in the deeper disk layers. This constant radiative flux through the disk atmosphere can be characterized by the effective temperature distribution of the steady optically-thick disk,

$$T_{eff}^4 = \frac{3GM\dot{M}}{8\pi\sigma R^3}\left[1-\left(\frac{R_i}{R}\right)^{1/2}\right]. \tag{1}$$

This equation predicts that the maximum disk temperature T_{max} occurs at $1.36R_i$ and then decreases to zero at $R = R_i$. The latter is unphysical, and so we modify equation (1) so that when the radius is smaller than 1.36 R$_i$, we assume that the temperature is constant and equal to $T = T_{max}$. (e.g., KHH88) The vertical temperature structure at each radius is calculated using the gray-atmosphere approximation in the Eddington limit, adopting the Rosseland mean optical depth τ.

The opacity of atomic and molecular lines has been calculated using the Opacity Distribution Function (ODF) method (Castelli & Kurucz 2004; Sbordone et al. 2004; Castelli 2005). Briefly, the ODF method is a statistical approach to handling line blanketing when millions of lines are present in a short wavelength range (Kurucz et al. 1974). For a given temperature and pressure, the absorption coefficient for each line is exactly computed, then the profiles of all the lines in each small interval $\Delta\nu$ are rearranged monotonically as a function of ν. The opacity increases as the frequency increases in this $\Delta\nu$. A step function with 12 subintervals in frequency is used to represent this monotonic function. The height of every step is the averaged opacity of the monotonic function in this subinterval. The width of the 12 subintervals are $\Delta\nu/10$ for 9 intervals and $\Delta\nu/20$, $\Delta\nu/30$, $\Delta\nu/60$ for the last 3 intervals where the monotonic function increases steeply and reaches the maximum. Thus, in every interval $\Delta\nu$ we obtain 12 representative averaged opacities at a given temperature and pressure. We then construct an opacity table as a function of λ for each temperature and pressure. The wavelength grid is the same as used in the code DFSYNTHE (Castelli 2005) from 8.976 nm to 10000 nm with 328 BIG intervals (resolution 30-100) and 1212 LITTLE intervals (resolution 60-500). However, we extend the temperature grid and pressure grid to lower temperatures and pressures ($\log T$ ranging from 1.5 to 5.3, $\log P$ from -24 to 8 in cgs units) than DFSYNTHE, so that it can be used in our disk models for which the temperatures and pressures reach lower values than in typical stellar atmosphere models. Because the line opacity usually varies by several orders of magnitude within a line width, the ODF method is substantially more accurate than either straight or harmonic means.

The line list is taken from Kurucz's CD-ROMs Nos. 1, 15, 24, and 26 (Kurucz 2005). Not only atomic lines but also many molecular lines (C_2, CN, CO, H_2, CH, NH, OH, MgH, SiH, SiO, TiO, H_2O) are included. The opacities of TiO and H_2O, the most important molecules in the infrared, are from Partridge & Schwenke (1997) and Schwenke (1998). We do not include a detailed calculation of the dust condensation process; instead, we add the dust opacity when T<1500 K (the condensation temperature of silicates at typical disk densities). We use the ISM dust model of Draine & Lee (1984, 1987) to represent the dust in the disk. This assumption is unlikely to be correct but mostly affects the continuum at the very longest wavelengths and in particular the silicate emission features, which we do not model in this paper.

At low temperatures complex chemical processes occur which are not included in the Kurucz data. We have not calculated the low temperature molecular opacity in detail; instead, we have assumed that the abundance ratio between different types of molecules below 700 K is the same as the ratio at 700 K. This is unimportant for our purposes because dust opacity dominates at such low temperatures.

In Figure 2 we show the Rosseland mean opacity calculated for solar abundances and a turbulent velocity $v = 2\,\mathrm{km\,s^{-1}}$ for different values of ρ/T_6^3 to be compared with Alexander & Ferguson (1994), where ρ is the density in $\mathrm{gcm^{-3}}$ and T_6 is the temperature in millions of degrees. The results closely match the more detailed calculations by Alexander & Ferguson (1994) and Ferguson et al. (2005) except near 1500 K, where our dust opacity rises more rapidly due to our neglect of dust condensation processes.

Calvet et al. (1991b) showed that the near-infrared spectrum of FU Ori could be well-modeled with the then-current water vapor opacities and a similar calculational method to the one we are using here. We now have a much better set of opacities, and can treat the optical spectrum. To test the code at optical wavelengths, we compare the model spectrum from the annulus with T$_{eff}$=5300 K with the observed spectrum of SAO 21446 which is a G1 supergiant (Jacoby et al. 1984). The spectrum of SAO 21446 has been obtained using the Intensified Reticon Scanner(IRS) on the No.1 90 cm telescope at Kitt Peak by Jacoby et al. (1984). Here we have convolved this spectrum to a resolution of 300 to agree with our model spectrum. As shown in Figure 3, our model reproduces the continuum spectrum fairly well except for a few strong features. These discrepancies are probably due to the limitation of the grey atmospheric assumption.

Figure 4 shows the emergent intensities with 55^o emergent angle from different annuli of our final disk model (parameters can be found in §4), which has 45 annuli. The 55^o inclination angle is estimated from the near-infrared interferometric observations by Malbet et al. (2005) and mid-infrared interferometric observations by Quanz et al. (2006). The radii of these annuli are chosen to increase exponentially from $r = R_i$ to $1000R_i$. At the first annulus ($r = 1R_i$), we can see a significant Balmer jump at 0.36 μm, similar to the spectra of early type stars. As the radius increases, the temperatures of the annuli become lower and lower. Infrared molecular features appear at larger annuli with effective temperatures less than 5000K ($r > 3R_i$). For the outermost annuli with effective temperature less than 1500 K ($r > 15R_i$), the molecular features have almost disappeared because dust opacity dominates. The final spectrum is the result of the addition of the fluxes from each of these annuli weighted by the appropriate annular surface area.

In addition to these calculations aimed at comparing with low-resolution spectra, we also calculated high-resolution spectra in restricted wavelength regions. For these calculations, the vertical structure of every annulus is calculated as above, and then this structure is imported into the program SYNTHE (Kurucz & Avrett 1981; Kurucz 1993). SYNTHE is a suite of programs which solve the radiative transfer equations in LTE with a very high spectrum resolution (∼500,000). Each annular spectrum is broadened with the rotational profile appropriate to a Keplerian disk and then the summed spectrum is calculated (e.g., KHH88). These calculations are very time-consuming, and were used only to produce a high resolution spectrum of a small wavelength range around 6170 Å for the purpose of estimating the central mass, and for examining the CO first-overtone lines.

4. Comparison with observations

The SED of a steady, optically-thick disk model is determined by two parameters: the product of the mass accretion rate and the mass of the central star, $\dot{M}M$, and the inner radius R_i. One observational constraint comes from the observed spectral lines and/or the peak of the SED (after reddening correction), which determines the maximum temperature of the steady disk model,

$$T_{max} = 0.488 \left(\frac{3GM\dot{M}}{8\pi R_i^3 \sigma} \right)^{1/4} . \tag{2}$$

The other observational constraint is given by the true luminosity of a flat disk L_d,

$$L_d = 2\pi d^2 \frac{F}{\cos i} = \frac{GM\dot{M}}{2R_i} , \tag{3}$$

where d is the distance of FU Ori, i is the inclination angle of the disk to the line of sight, and F is the observed total flux corrected for extinction. If the distance and inclination are known, we can solve for the inner disk radius and thus for the product $M\dot{M}$. If we then further use the observed rotational velocities, it is then possible to derive independent values of the central mass M and the accretion rate $\dot{M}$, in the manner outlined by KHH88.

The best constraints on T_{max} come from the optical spectrum, as the uncertain extinction makes it difficult to constrain by overall SED fitting. From the lines of our optical FAST spectrum we derive a spectral type of $\sim$ G2 for FU Ori using the methods of Hernández et al. (2004), which agrees with previous results (Herbig 1977). However, it is not straightforward to derive a value of extinction and thus T_{max} from this spectral type determination; the disk spectrum is not that of a single (standard) star with a well-defined effective temperature, but instead it is a combination of hotter and cooler regions, with an overall spectrum that clearly varies with the wavelength of observation in a complicated way. To address this problem, we constructed several disk models with a modest range of T_{max} and compared them with the observed optical spectrum dereddened by differing amounts of visual extinction A_V, as shown in Figure 5.

The uppermost model in Figure 5 has T_{max} = 7240 K, comparable to that of the FU Ori disk model of KHH88. The model optical spectrum is too flat longward of $\sim$ 3900 Å in comparison with the observations dereddened by the $A_V = 2.2$, suggested by KHH88, or for $A_V = 1.9$. At the other extreme, we find that the bottom model, with T_{max} = 5840 K, matches the observed spectrum dereddened by only $A_V = 1.3$ quite well. However, we suspect that our gray-atmosphere approximation somewhat underestimates the amount of line blanketing in the blue optical region, especially shortward of the Ca II resonance lines at 3933 and 3968 Å leading us to suspect that this agreement is somewhat misleading. We therefore provide our best estimate of the extinction as $A_V = 1.5 \pm 0.2$, and adopt the model which best matches the mean extinction with T_{max} = 6420 K as our standard model.

In this connection it is worth noting that KHH88 did not actually find a good fit for the optical spectrum of FU Ori using a G0I standard star and extinctions $A_V > 2$. They speculated that the discrepancy might be alleviated by an improved treatment of limb darkening in the disk. However, Hartmann & Kenyon (1985) had found that a G2I standard star and $A_V = 1.55$ provided a good match to the optical spectrum between 3900 Å and 7400 Å , consistent with our results here.

The accretion disk luminosity L depends upon the distance, inclination, and dereddened flux. We adopt a distance of $\sim$ 500 pc, consistent with membership in the general Orion region (Herbig 1977). The inclination 55^o is adopted (Malbet et al.2005, Quanz et al. 2006). Using these parameters, observed total flux and $A_V = 1.5$, we obtain the true luminosity $L_d = 8.66 \times 10^{35} \mathrm{ergs\,s^{-1}} {\sim} 226 L_\odot$ according to equation 3. As mentioned before, fitting the observed spectrum yields $T_{max} = 6420$ K. We derive $M\dot{M} = 7.2 \times 10^{-5} M_\odot^2 \mathrm{yr}^{-1}$ and $R_i = 5R_\odot$ by solving equation 2 and equation 3 simultaneously.

Figure 6 shows the predicted spectrum for the adopted parameters and several values of the outer radius. Our computed spectrum matches the observations at wavelengths shortward of about 4μm, indicating that the innermost region of the inner disk is reasonably well reproduced by the adopted $\dot{M}M$ and R_i parameters.

Because the optical and near-infrared SED is well-matched by the model, we may then proceed to estimate the central stellar mass and thus the accretion rate. We used the observed optical rotation from KHH88 to constrain the central star mass. We computed the line profiles around 6170 $\dot{A}$ using SYNTHE, cross correlated it with a non-rotating disk spectrum, and compared it with the observed cross-correlation line profile given in KHH88. The uncertainty in fitting the line profile widths is about ± 20%. However, systematic errors in the inclination angle are probably more important for the mass estimate, and for that reason we give an uncertainty $0.3M_\odot \pm 0.1M_\odot$ (consistent with the earlier estimate of KHH88 assuming $i = 50°$). For a mass of 0.3 $M_\odot$, $\dot{M} \sim 2.4 \times 10^{-4} M_\odot \mathrm{yr}^{-1}$. Parameters of the model are given in Table 1.

As shown in Figure 6, we find that regardless of extinction and disk parameters, steady accretion models which fit the optical to near-infrared region predict too much emission in the IRS range for very large outer radii. This can only be remedied by truncating the hot inner disk. The estimate of the outburst models of Bell & Lin (1994) suggested an outer radius of the high state of $\sim 20\mathrm{R}_\odot$ (with somewhat different parameters for the accretion rate and inner disk radius); as shown in Figure 6 this truncation radius fails to explain the SED. A truncation radius of $R_{out} \sim 210 R_\odot \sim 1$ AU provides a better fit to the flux at $\sim 5 - 8\mu$m, although is somewhat low in the 3μm band. Our results are reasonably consistent with Green et al. (2006), considering the limitations of their blackbody modeling only out to 5 microns.

As discussed above, models with outer radii larger than ${\sim}200 R_\odot$ overpredict the flux at

$\sim 5-8\mu$m. At even longer wavelengths, absorption features are no longer present; instead, silicate dust emission features are seen in IRS spectra at $\sim$ 10 and 20μm. As discussed by Green et al. (2006), these silicate features are signatures of heating from above, rather than from internal viscous dissipation, and may be produced in upper atmosphere of the outer disk which absorb light from the central disk. An outer disk is expected to be present, since a disk radius of $\sim 0.5-1$ AU is extremely small by standards of typical T Tauri disks, for which $R_{out} \sim 100$ AU or more are common (e.g., Simon, Dutrey, & Guilloteau 2000). Moreover, such a small radius would imply a low-mass optically-thick disk, making it difficult to explain the observed submm flux from FU Ori (Sandell & Weintraub 2001). So, it is very likely that an outer disk is present with a lower accretion rate, which could contribute some flux in the $5-8\mu$m wavelength range and thus reduce the radius of the hot, high-accretion rate region. An outer disk accretion rate of about 10^{-5}M$_\odot$ yr^{-1} is comparable to some of the highest infall rates estimated for (not heavily embedded) protostars (e.g., Kenyon, Calvet & Hartmann 1993); higher accretion rates would imply implausibly short evolutionary timescales $M/\dot{M} \sim 3 \times 10^4$ yr. In any event, if the outer disk accretion rate is not significantly smaller than the inner disk accretion rate, the problem of a large outer radius yielding too much flux remains. More likely, the emission from the outer disk is dominated by irradiation from the inner disk independent of the (lower) accretion rate there (Turner et al. 1997), as indicated by the presence of emission rather than absorption features.

In the Bell & Lin (1994) thermal instability models for FU Ori outbursts, the outer disk accretion rate is of order 10^{-1} of the inner disk accretion rate in outburst. We have therefore investigated the effect of an outer disk accretion rate of 2.4×10^{-5}M$_\odot$ yr^{-1} on the SED. The dotted curves in Figure 6 show the results of adding in such outer disk emission from disk internal viscous dissipation. The effect is relatively small so that our estimate of the outer radius of the hot disk with the high accretion rate is relatively robust. Of course we cannot rule out other kinds of temperature distributions, such as a smooth decline of accretion rate from, say, 100 to 200 R$_\odot$ and the irradiation effect from the inner disk to the outer disk. We are presently carrying out more detailed calculations of the outer disk, including irradiation by the inner disk. Preliminary results indicate that the addition of the irradiated outer disk emission will decrease our hot disk outer radius estimate by no more than a factor of two (Zhu et al., in preparation).

We explored the effects of a larger visual extinction by scaling the observations to A$_V$=2.2. As shown in Figure 7, this makes only a very slight difference to the long-wavelength spectrum and does not change our estimate of the outer radius.

To examine our consistency with previous results, we calculated the CO first overtone high resolution spectrum with $R_{out} = 210 R_\odot$ using SYNTHE program and compared it with the high resolution spectrum from Hartmann et al. (2004). The comparison is shown in Figure 8. We found that we needed to adopt a turbulent velocity of 4 $\mathrm{km\,s^{-1}}$ to obtain lines that are deep enough in comparison with the observations. This is the sound speed of gas with temperature around 4000 K, slightly supersonic for the annulus with radius larger than 4 stellar radius; Hartmann, Hinkle, & Calvet (2004) similarly found that slightly supersonic turbulence was needed to explain the first-overtone CO lines, and pointed out that this would not be surprising in the context of turbulence driven by the magnetorotational instability.

In Figure 9 we show an expanded view of the wavelength region between $\sim$ 3 and 8μm. The model accounts for the overall shape of the SED reasonably well, and yields a reasonable strength for the 6.8μm water vapor absorption feature. However, the 5.8μm water vapor feature of the model is not as strong as it is in the observations ((Green et al. 2006)). In this wavelength region the contributions from the dust-dominated regions of the disk are significant, and the contribution of this dust (relatively featureless) continuum emission could reduce the strength of the absorption feature. To investigate this possibility, we reduced the dust opacity to only 1% that of Draine & Lee (1984, 1987) and recalculated the model (with a slightly larger outer radius). As can be seen in Figure 9, this reduction in dust opacity strengthens the absorption features, although the predicted 5.8μm feature is still not strong enough, perhaps suggesting some difficulty with the opacities. It is not clear whether we require dust depletion, because we have not considered the temperature dependence of dust condensation in our model. We also cannot rule out uncertainties due to our simple treatment of the vertical temperature structure of the disk.

5. Discussion

5.1. The steady accretion disk model and the inner boundary condition

We have shown that the steady accretion disk model can quantitatively account for the observed SED of FU Ori over a factor of nearly 20 in wavelength, from 4000 Å to about 8μm. This is accomplished with only three adjustable parameters: R_i, $\dot{M}M$, and R_{out}. No alternative model proposed for FU Ori has explained the SED over such a large wavelength range. The accretion disk explanation is bolstered by this work.

Within the context of the steady disk model, however, there remains the question of the appropriate inner boundary condition. The steady disk model considered here only accounts for half of the accretion luminosity ($L = G\dot{M}M/(2R_i)$) potentially available from accretion onto a slowly rotating star. As Kenyon et al. (1989) showed from ultraviolet spectra, there is no evidence in FU Ori for boundary layer emission which would account for this missing luminosity, up to $\sim$ 10-20% of the total luminosity; and if our lower estimate of extinction is correct, the potential boundary layer emission would be much less. This leaves as possibilities that the missing accretion energy is going into spinning up the central star, expanding the central star, being radiated over a larger radial distance of the disk, or some combination of all three effects.

Hartmann & Kenyon (1985; also Kenyon et al. 1989) pointed out that the 5 $R_\odot$ inner radius implied by steady disk models is considerably larger than that of the typical T Tauri star ($R \sim 2R_\odot$), and suggested that this might be due to the disk dumping large amounts of thermal energy into the star, expanding its outer layers.

Popham et al. (1993, 1996) suggested that the the missing boundary layer energy could be distributed over a significant range of radii in the disk at high accretion rates. They found that as $\dot{M}$ increases to $\sim 10^{-4}$ $M_\odot yr^{-1}$ the dynamical boundary layer (the radial extent of the region where Ω drops from Keplerian angular velocity to 0) grows to 10-20 % of a stellar radius and the thermal boundary layer (the radial width over which the boundary layer luminosity is radiated) grows to the point that it becomes impossible to distinguish the boundary layer from the inner parts of the disk. Popham et al. (1996) showed that this model would imply somewhat slower than Keplerian rotation in the innermost disk. In this paper we find no evidence for extra radiation if A_V=1.5. We cannot rule out a slightly larger A_V, which would allow some extra dissipation of kinetic energy in the inner disk. However, the shape of the spectrum in the blue-optical region (Figure 5) suggests that the higher extinction value is not preferred, limiting the amount of excess radiation to a modest fraction of the total luminosity. We speculate that the missing energy is mostly going into expanding the outer stellar layers, with perhaps a small amount of excess radiation that is difficult to discern given the uncertainties in the extinction.

5.2. R_{out} and α

Our estimate of the outer radius of the high state of FU Ori is around 200 $R_\odot$, although the irradiation effect from the hot inner disk to the outer disk may decrease this value to no less than 100 $R_\odot$. Bell & Lin (1994) assume low viscosity parameters ($\alpha \sim 10^{-3}$) and derive a small outer radius ($R_{out} \sim 20 R_\odot$) for the high $\dot{M}$, hot inner disk during outbursts. Our model of FU Ori is inconsistent with such a small hot region; instead, we require the high $\dot{M}$ region to be an order of magnitude larger in radius.

FU Ori has been fading slowly in brightness over the last $\sim$ 70 years (Ibrahimov 1999). If we attribute this fading to the emptying out of mass from the inner hot disk onto the central star, this timescale gives us a way to constrain the viscosity in this region. We make the simple assumption that the decay timescale is the viscous timescale

$$t_v \sim R^2/\nu\,, \tag{4}$$

where the viscosity is $\nu = \alpha c_s^2/\Omega$, α is the viscosity parameter (Shakura & Sunyaev 1973), c_s is the sound speed in the disk midplane, and Ω is the Keplerian angular frequency at R. We use the isothermal sound speed with a mean molecular weight of 2.3, appropriate for molecular hydrogen. We then need an estimate of the central temperature to evaluate t_v. Our radiative transfer model shows that the effective temperature is $T_{eff} \sim 800$ K at the outer radius of $R \sim 200\mathrm{R}_\odot$. This is a lower limit for the central temperature as the absorption features in the spectrum show that the central temperature is higher than the surface temperature. The disk is likely to be very optically thick in this region, such that the central temperature is considerably larger than the effective temperature due to radiative trapping. We choose 1500 K as the central temperature above which MRI is active and thus high α can sustain high mass accretion rate. We therefore find

$$t_v \sim 141\,\mathrm{yrs} \times \left(\frac{M}{0.3M_\odot}\right)^{1/2} \left(\frac{R}{210R_\odot}\right)^{1/2} \left(\frac{T}{1500K}\right)^{-1} \left(\frac{\alpha}{10^{-1}}\right)^{-1}\,. \tag{5}$$

where M is the mass of the central star, R is the outer radius of the high mass accretion disk, T is the central disk temperature of the high mass accretion disk, and α is the viscosity parameter. If we estimate a typical decay timescale of FU Ori as ~ 100 yr, then we find $\alpha \sim 0.14$. For the smaller hot disk radius with an irradiated outer disk, our preliminary results yield (Zhu et al., in preparation) R $\geq$0.5 AU and thus $\alpha \sim 0.1$.

It is important to recognize that equation (5) is only an order of magnitude estimate. The decay timescale of accretion can be affected by whatever mechanism makes the transition from high to low state; for example, in the thermal instability model, the decay time may not be the timescale for emptying out half the material in the affected region of the disk, but only that (smaller) amount necessary to shut off the thermal instability. Nevertheless, it is suggestive that we find a larger value of α in the high state than the 10^{-3} of Bell & Lin (1994).

A value of $\alpha \sim 0.2 - 0.02$ is roughly consistent with estimates from compact systems with accretion disks (King et al. 2007) as well as with numerical simulations of the magnetorotational instability (MRI) in ionized disks (Balbus & Hawley 1988). In this connection, we note that the requirement for enough thermal ionization to initiate a robust MRI is a central temperature $T \gtrsim 1000$ K (Gammie 1996), comparable to our observationally-based estimates ($T_{eff}$$\sim$800 K at $R \sim 200$ R$_\odot$).

5.3. Thermal and other instabilities

The thermal instability model was originally suggested to account for outbursts in dwarf nova systems (Faulkner, Lin, & Papaloizou 1983) and has attractive properties for explaining FU Ori outbursts (Bell & Lin 1994). However, the observed large outer radius, $0.5 - 1$ AU, of the high accretion rate portion of the FU Ori disk poses difficulties for the pure thermal instability model. Even in the situation explored by Lodato & Clarke (2004), in which the thermal instability is triggered by a massive planet in the inner disk, the outer radius of the high state is still the same as in Bell & Lin (1994), $\sim 20\ \mathrm{R}_\odot$. The relatively high temperatures ($2-4\times10^3$ K) required to trigger the thermal instability (due to the ionization of hydrogen) are difficult to achieve at large radii; they require large surface densities which in turn produce large optical depths, trapping the radiation internally and making the central temperature much higher than the surface (effective) temperature.

To illustrate the problem, we calculated thermal equilibrium "S" curves (e.g., Faulkner et al. 1983) for our disk parameters at $R = 210\mathrm{R}_\odot$ but various values of α. The equilibrium curve represents energy balance between viscous energy generation and radiative losses,

$$F_{vis} = F_{rad} \tag{6}$$

Thus,

$$\frac{9}{4}\alpha\Omega\Sigma c_s^2 = 2\sigma T_{eff}^4\,, \tag{7}$$

where Σ is the surface density and c_s is the sound speed at the local central disk. For an optically-thick disk, we have $\mathrm{T}_c^4{=}\frac{3}{8}\tau_R\mathrm{T}_{eff}^4$, where $\tau_R{=}\kappa_R\Sigma$ and κ is the Rosseland mean opacity (Hubeny 1990). Then,

$$T_c^3 = \frac{27}{64\mu\sigma}\alpha\Omega\Sigma^2\mathcal{R}_c\kappa\,, \tag{8}$$

where $\mathcal{R}_c$ is the gas constant, and μ is the mean molecular weight . As long as we know T_c, we can derive T_{eff} and the corresponding $\dot{M}$ at this radius. Because the Rosseland mean opacity is also dependent on temperature and pressure, iteration of the disk structure calculation is needed to derive the equilibrium curve.

We show in Figure 10 the equilibrium curve at R=210 $\mathrm{R}_\odot$ for five values of α: 10^{-1}, 10^{-2}, 10^{-3}, 10^{-4}, 10^{-5}. In discussing our results, we define Σ_A to be the highest stable low state for a given α. If at any radius the surface density increases above Σ_A, the disk can no longer stay stable on the lower branch and strong local heating begins. If the α of the low state is the same as the α of the high state, then $\alpha{\geq}10^{-2}$; in this case, to trigger the thermal instability at Σ_A, the mass accretion rate in the low state would need to be $\sim10^{-3}$

(see Figure 10), which is higher than the $\dot{M}$ of the high state that we have determined. To have a mass accretion in the low state at least one order of magnitude lower than that of the high state, we would need $\alpha \leq 10^{-4}$ for the low state (see Figure 10). This is comparable to the low state α used by Bell & Lin (1994), but very much lower than our high state estimate. Changing the outer radius to R$\sim$100 $R_\odot$ does not change these results by more than a factor of 10.

With $\alpha = 10^{-4}$, the critical surface density at 210 $R_\odot$ is $\Sigma_A \sim 10^6$ g cm^{-2}. Then we can estimate the Toomre Q parameter,

$$Q = \frac{c_s \Omega}{\pi G \Sigma_A} \sim 0.1\,, \tag{9}$$

where $Q < 1$ implies gravitational instability. Thus, a thermal instability model for FU Ori implies a massive, probably gravitationally-unstable disk, which raises the question: could the outburst be driven by gravity instead?

Armitage et al. (2001) proposed an alternative model of disk outbursts in which material piles up at radii of order 1-2 AU, consistent with layered disk models (Gammie 1996), achieving repeated outbursts with high accretion on size scales much closer to our inferred R_{out}. In this model, gravitational torques lead to increased accretion, which in turn heats up the inner disk until temperatures are high enough (800 K in their model) to trigger the MRI, which results in very much higher viscosities and rapid accretion. The Armitage et al. (2001) model does not give exactly FU Ori-type outbursts; instead, the accretion events last for $\sim 10^4$ yr and achieve peak accretion rates of only $\sim 10^{-5} M_\odot\,\mathrm{yr}^{-1}$. However, Armitage et al. (2001) suggested that thermal instabilities might be triggered by their gravitationally-driven outbursts. Simple models with somewhat different parameters demonstrate that it is indeed possible to trigger thermal instabilities in the context of this general model (Gammie, Book, & Hartmann 2007, in preparation), resulting in outbursts more similar to that of FU Ori.

Vorobyov & Basu (2005,2006) suggest FU Ori outburst could be explained by the accretion of clumps formed in a gravitationally unstable disk. The disk becomes gravitationally unstable because of the infall of the matter from the envelope. The spiral arms and clumps form and grow in the unstable disk. The redistribution of mass and angular momentum leads to centrifugal disbalance in the disk and further triggers the outburst when the dense clumps are driven into the central star. The authors derive a mass accretion rate at 10 AU of $\sim 10^{-4} M_\odot$/yr, which could result in too much emission from the outer disk; this issue requires further exploration.

The rapid rise time of the outburst of FU Ori in the B band, $\sim$ 1 year, provides the best evidence for a thermal instability. We can test this idea very crudely by using our steady disk model to estimate the range of radii in the disk which can contribute to the B band magnitude in the light curve, finding that only the inner $R \lesssim 20\mathrm{R}_\odot$ disk are involved. If we then assumed that the rise in B light is due to the inward propagation of a thermal instability front across this region at a (maximum) speed $\sim \alpha c_s$ (Lin et al. 1985; Bell et al. 1995), and assume a sound speed characteristic of $2-4\times10^3$ K (the minimum temperature for instability), then we derive $\alpha \sim 0.1$. While this calculation is very crude, it does suggest consistency with the idea of a thermal instability with a viscosity parameter comparable to that which we inferred from the decaying light curve (§5.2).

Finally, we estimate the amount of mass in the inner disk. An upper mass limit for the inner disk can be estimated by assuming Q $\sim$ 1 (the approximate limit for strong gravitational instability) at $R \sim 200$ R$_\odot$. Adopting a central temperature $T \sim 1000$ K, the gravitational instability limit leads to an approximate surface density limit $\Sigma \lesssim 10^5 gcm^{-2}$ and thus a maximum inner disk mass $\sim \pi\Sigma R^2 \sim 0.05\mathrm{M}_\odot$. This leads us to an inner disk mass estimate $0.05\mathrm{M}_\odot \gtrsim \mathrm{M}_{\mathrm{in}} \gtrsim 0.01\mathrm{M}_\odot$, where the lower limit comes from requiring the outburst mass accretion rate of $\sim 10^{-4}\mathrm{M}_\odot\,\mathrm{yr}^{-1}$ to be sustained for the observed decay timescale of $\sim$ 100 yr.

6. Conclusions

Using the latest opacities and the ODF method, we have constructed a new detailed radiative transfer disk model which reproduces the main features of the FU Ori spectrum from $\sim 4000\dot{A}$ to about 8 μm. The SED of FU Ori can be fitted with a steady disk model and no boundary layer emission if A$_V$$\sim$1.5, a somewhat lower valued extinction than previously estimated. A larger A$_V$ would imply extra heating at small radii which would result from dissipation of kinetic energy as material accretes onto the central star. With A$_V$=1.5, the inclination estimated from near-IR interferometry and the observed rotation of the inner disk, we estimate that the central star has a mass $\sim 0.3M_\odot$ (typical of low-mass TTS) and a disk mass accretion rate of $\sim 2.4\times10^{-4}\mathrm{M}_\odot\,\mathrm{yr}^{-1}$.

Relying on the Infrared Spectrograph Spectrum of FU Ori from the Spitzer Space Telescope presented by Green et al. (2006), we estimate that the outer radius of the hot, rapidly accreting region of the inner disk is $\sim$1 AU, although the irradiation effect may decrease this value by no more than a factor of two(Zhu et al., in preparation). Either way, this is inconsistent with the pure thermal instability models of Bell & Lin (1994) who adopted a low α viscosity parameter $\sim$10^{-3}-10^{-4}. If we assume that the observed decay timescale of FU Ori ($\sim$100 years) is the viscous transport time from the outer edge of the hot region, then we derive $\alpha \sim 0.2-0.02$, , comparable to the predictions of simulations of the magnetohydrodynamic (MHD) turbulence. The effective temperature at the outer edge of the hot region in our model is $\sim$800 K ; the presence of absorption features shows that the central disk temperature must be higher. Thus, our model suggests that the central disk temperature is greater than the $T_c \sim 1000$ K required to maintain full MHD turbulence by thermal ionization out to $\sim$ 1 AU.

We show that pure thermal instability models have difficulty in explaining the outburst of FU Ori, and suggest that models including gravitational torques and MRI activation, such as those of Armitage et al. (2001), are more promising.

We thank Dr. R. Kurucz and Dr. F. Castelli for making their line list and ATLAS codes available. They also provide us very helpful suggestions to help us run their codes smoothly. We also thank Mansur Ibrahimov for communicating recent photometry of FU Ori and Thomas P. Greene for providing the near-infrared spectrum of FU Ori. This work was supported in part by NASA grant NNG06GJ32G and the University of Michigan.

REFERENCES

Alexander, D. R., & Ferguson, J. W. 1994, ApJ, 437, 879

Armitage, P. J., Livio, M., & Pringle, J. E. 2001, MNRAS, 324, 705

Aspin, C., & Reipurth, B. 2003, AJ, 126, 2936

Balbus, S. A., & Hawley, J. F. 1998, Reviews of Modern Physics, 70, 1

Bell, K. R., & Lin, D. N. C. 1994, ApJ, 427, 987

Bell, K. R., Lin, D. N. C., Hartmann, L. W., & Kenyon, S. J. 1995, ApJ, 444, 376

Calvet, N., Hartmann, L., & Kenyon, S. J. 1991, ApJ, 383, 752

Calvet, N., Patino, A., Magris, G. C., & D'Alessio, P. 1991, ApJ, 380, 617

Castelli, F. 2005, Memorie della Societa Astronomica Italiana Supplement, 8, 34

Castelli, F., & Kurucz, R. L. 2004, ArXiv Astrophysics e-prints, arXiv:astro-ph/0405087

Clarke, C., Lodato, G., Melnikov, S. Y., & Ibrahimov, M. A. 2005, MNRAS, 361, 942

Cohen, M., Wheaton, W. A., & Megeath, S. T. 2003, AJ, 126, 1090

Cohen, M., & Woolf, N. J. 1971, ApJ, 169, 543

Draine, B. T., & Lee, H. M. 1984, ApJ, 285, 89

Draine, B. T., & Lee, H. M. 1987, ApJ, 318, 485

Fabricant, D., Cheimets, P., Caldwell, N., & Geary, J. 1998, PASP, 110, 79

Faulkner, J., Lin, D. N. C., & Papaloizou, J. 1983, MNRAS, 205, 359

Ferguson, J. W., Alexander, D. R., Allard, F., Barman, T., Bodnarik, J. G., Hauschildt, P. H., Heffner-Wong, A., & Tamanai, A. 2005, ApJ, 623, 585

Gammie, C. F. 1996, ApJ, 457, 355

Gammie, C. F. 1999, ASP Conf. Ser. 160: Astrophysical Discs - an EC Summer School, 160, 122

Green, J. D., Hartmann, L., Calvet, N., Watson, D. M., Ibrahimov, M., Furlan, E., Sargent, B., & Forrest, W. J. 2006, ApJ, 648, 1099

Greene, T. P., & Lada, C. J. 1996, AJ, 112, 2184

Goodrich, R. W. 1987, PASP, 99, 116

Hartmann, L., Hinkle, K., & Calvet, N. 2004, ApJ, 609, 906

Hartmann, L., & Kenyon, S. J. 1985, ApJ, 299, 462

Hartmann, L., & Kenyon, S. J. 1987a, ApJ, 312, 243

Hartmann, L., & Kenyon, S. J. 1987b, ApJ, 312, 243

Hartmann, L., & Kenyon, S. J. 1991, IAU Colloq. 129: The 6th Institute d'Astrophysique de Paris (IAP) Meeting: Structure and Emission Properties of Accretion Disks, 203

Hartmann, L., & Kenyon, S. J. 1996, ARA&A, 34, 207

Herbig, G. H. 1977, ApJ, 217, 693

Hernández, J. 2005, Ph.D. Thesis, Postgrado de Física Fundamental, Universidad de Los Andes, Venezuela.

Hernández, J., Calvet, N., Briceño, C., Hartmann, L., & Berlind, P. 2004, AJ, 127, 1682

Hubeny, I. 1990, ApJ, 351, 632

Ibrahimov, M. A. 1999, Informational Bulletin on Variable Stars, 4691, 1

Jacoby, G. H., Hunter, D. A., & Christian, C. A. 1984, ApJS, 56, 257

Kenyon, S. J., & Hartmann, L. W. 1991, ApJ, 383, 664

Kenyon, S. J., Hartmann, L., Gomez, M., Carr, J. S., & Tokunaga, A. 1993, AJ, 105, 1505

Kenyon, S. J., Hartmann, L., & Hewett, R. 1988, ApJ, 325, 231 (KHH88)

Kenyon, S. J., Hartmann, L., Imhoff, C. L., & Cassatella, A. 1989, ApJ, 344, 925

King, A. R., Pringle, J. E., & Livio, M. 2007, MNRAS, 376, 1740

Kurucz, R. L. 1993, Kurucz CD-ROM, Cambridge, MA: Smithsonian Astrophysical Observatory, —c1993, December 4, 1993,

Kurucz, R. L. 2005, Memorie della Societa Astronomica Italiana Supplement, 8, 86

Kurucz, R. L., & Avrett, E. H. 1981, SAO Special Report, 391,

Kurucz, R. L., Peytremann, E., & Avrett, E. H. 1974, Washington : Smithsonian Institution : for sale by the Supt. of Docs., U.S. Govt. Print. Off., 1974., 37

Lin, D. N. C., Faulkner, J., & Papaloizou, J. 1985, MNRAS, 212, 105

Lodato, G., & Clarke, C. J. 2004, MNRAS, 353, 841

Malbet, F., et al. 2005, A&A, 437, 627

Mould, J. R., Hall, D. N. B., Ridgway, S. T., Hintzen, P., & Aaronson, M. 1978, ApJ, 222, L123

Muzerolle, J., Calvet, N., Hartmann, L., & D'Alessio, P. 2003, ApJ, 597, L149

Papaloizou, J., Faulkner, J., & Lin, D. N. C. 1983, MNRAS, 205, 487

Partridge, H., & Schwenke, D. W. 1997, J. Chem. Phys., 106, 4618

Popham, R., Narayan, R., Hartmann, L., & Kenyon, S. 1993, ApJ, 415,

Popham, R., Kenyon, S., Hartmann, L., & Narayan, R. 1996, ApJ, 473, 422

Quanz, S. P., Henning, T., Bouwman, J., Ratzka, T., & Leinert, C. 2006, ApJ, 648, 472L127

Rayner, J. T., Toomey, D. W., Onaka, P. M., Denault, A. J., Stahlberger, W. E., Watanabe, D. Y., & Wang, S.-I. 1998, Proc. SPIE, 3354, 468

Reipurth, B., & Aspin, C. 1997, AJ, 114, 2700

Reipurth, B., & Aspin, C. 2004, ApJ, 608, L65

Sandell, G., & Aspin, C. 1998, A&A, 333, 1016

Sandell, G., & Weintraub, D. A. 2001, ApJS, 134, 115

Sbordone, L., Bonifacio, P., Castelli, F., & Kurucz, R. L. 2004, Memorie della Societa Astronomica Italiana Supplement, 5, 93

Schwenke, D. W. 1998, Chemistry and Physics of Molecules and Grains in Space. Faraday Discussions No. 109, 321

Shakura, N. I., & Sunyaev, R. A. 1973, A&A, 24, 337

Simon, M., Dutrey, A., & Guilloteau, S. 2000, ApJ, 545, 1034

Turner, N. J. J., Bodenheimer, P., & Bell, K. R. 1997, ApJ, 480, 754

Vorobyov, E. I., & Basu, S. 2005, ApJ, 633, L137

Vorobyov, E. I., & Basu, S. 2006, ApJ, 650, 956

This preprint was prepared with the AAS LaTeX macros v5.2.

Table 1: Best fit model

$M_{star}/M_\odot$	$\dot{M}$	$R_i/R_\odot$	$R_{out}/R_\odot$	θ[a]	Distance/pc
0.3	$2.4\times10^{-4} M_\odot$/yr	5	210	55^o	500

---

[a] Inclination angle of the disk from Malbet et al. (2005)

Table 2: Optical lines used to determine the spectral type

Lines [a]	Metals	Spectral type
4047.00	Fe I+Sc I	F8
4226.00	Ca I	G1
4271.00	Fe I	G4
4305.00	CH(Gband)	G1
4458.00	Mn I+Fe I	G1
5329.00	Fe I	G2
5404.00	Fe I	G3
6162.00	Ca I+TiO	F9

---

[a] From Hernandez (2005)

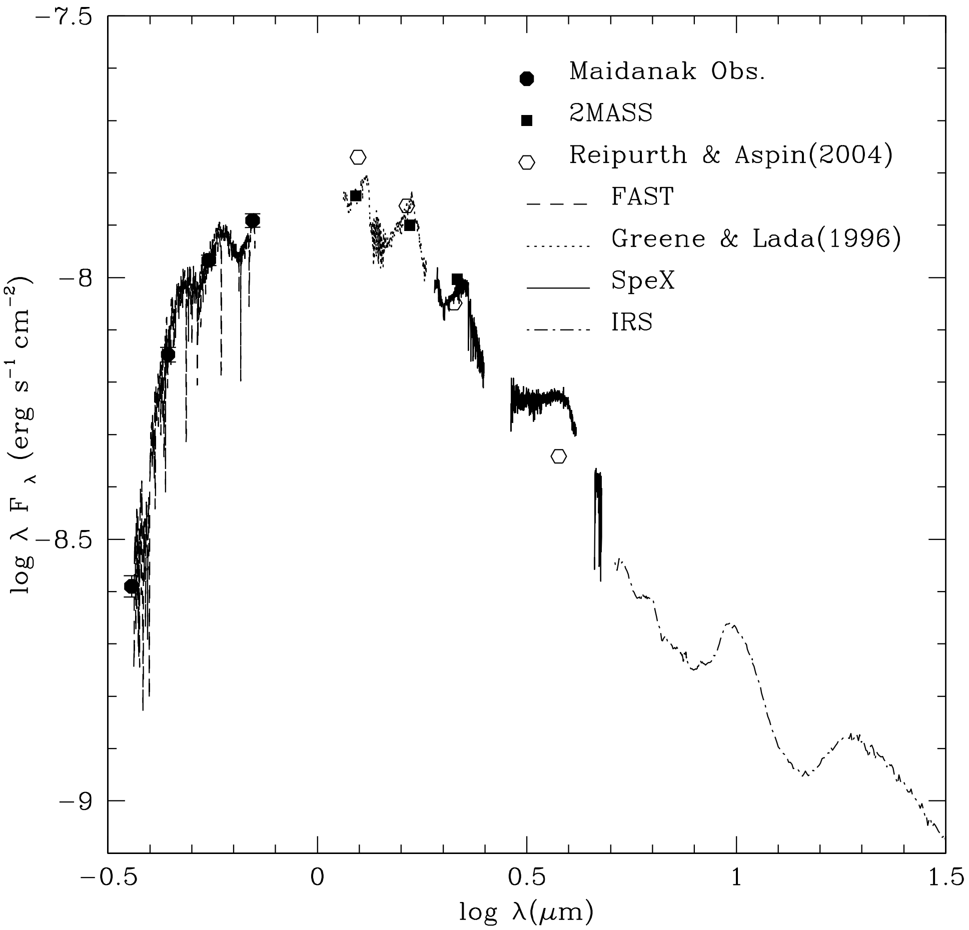

Fig. 1.— The spectral energy distribution of FU Ori. Collected photometric and spectroscopic data of FU Ori with A_v=1.5 (see §4). The solid circles with error bars are the UBVR photometry from the Maidanak Observatory, the squares are 2MASS JHK photometry, and the open circles are JHK'L' photometry from Reipurth & Aspin (2004). The dashed curve is the FAST spectrum from 3650 Å to 7500 Å, the dotted curve is the KSPEC spectrum from 1.15 μm to 2.42 μm (Greene & Lada 1996), and the solid curve is the SpeX spectrum from 2.1 μm to 4.8 μm (Muzerolle et al. 2003), both scaled to the 2MASS photometry. Finally, the dot-dash curve is the IRS spectrum from 5 μm to 35 μm from Green et al. (2006). The spectra were put on as absolute flux scale as discussed in §2.

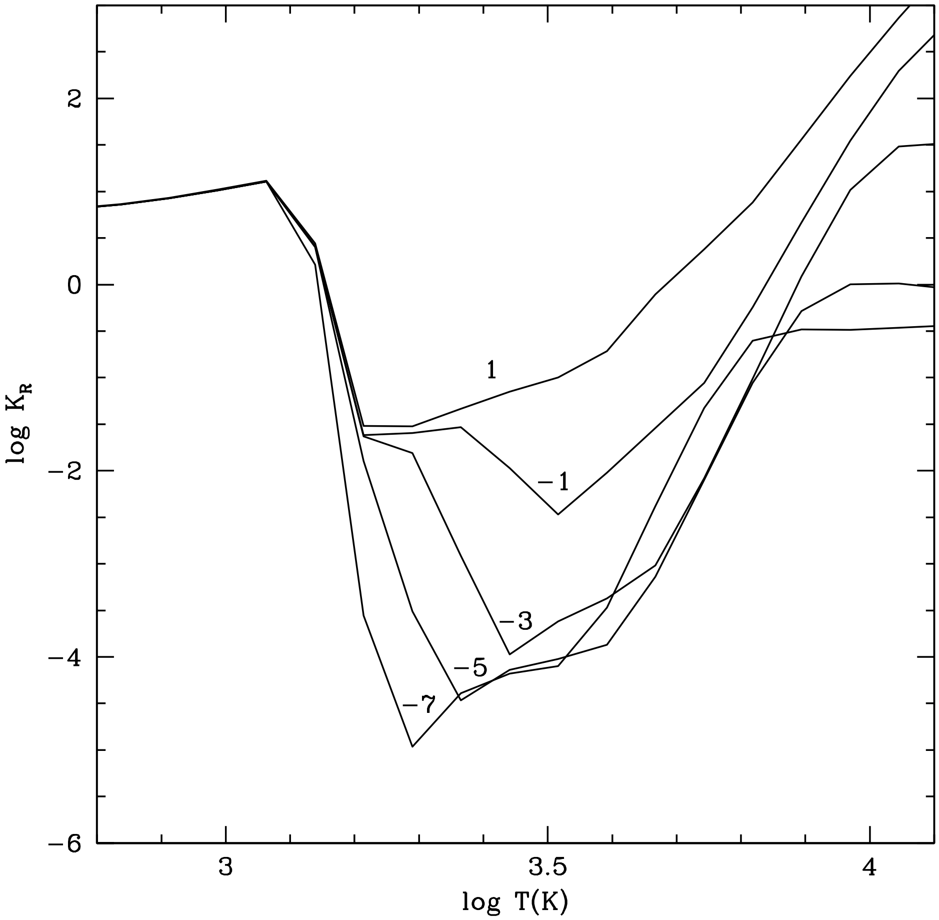

Fig. 2.— Our calculated Rosseland mean opacity as a function of temperature for solar composition. Each curve is labeled with the value of $\log(\rho/T_6^3)$ to be compared with Alexander & Ferguson (1994), where T_6 is the temperature in millions of degrees.

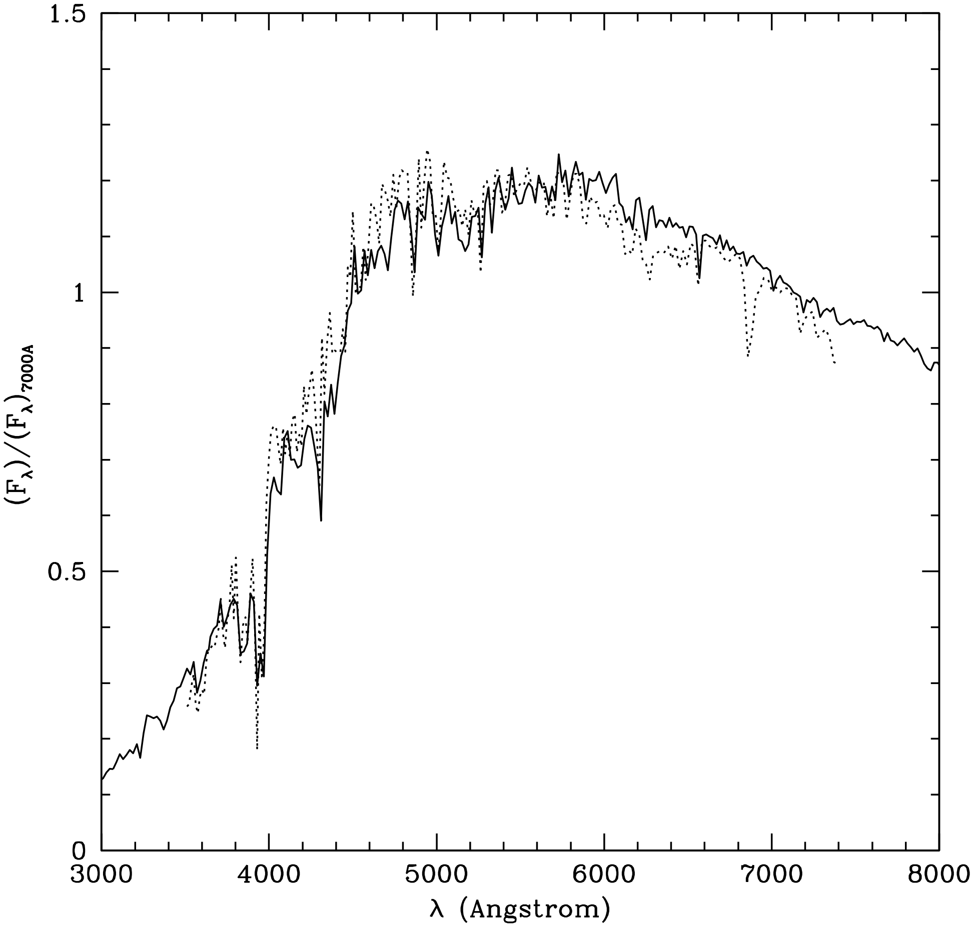

Fig. 3.— The spectrum predicted by the annulus with T_{eff}=5300 K (solid line) and the spectrum of SAO 21446 which is a G1 I star (Jacoby et al. 1984) (dotted line). The spectra are scaled to the same flux at 7000 Å.

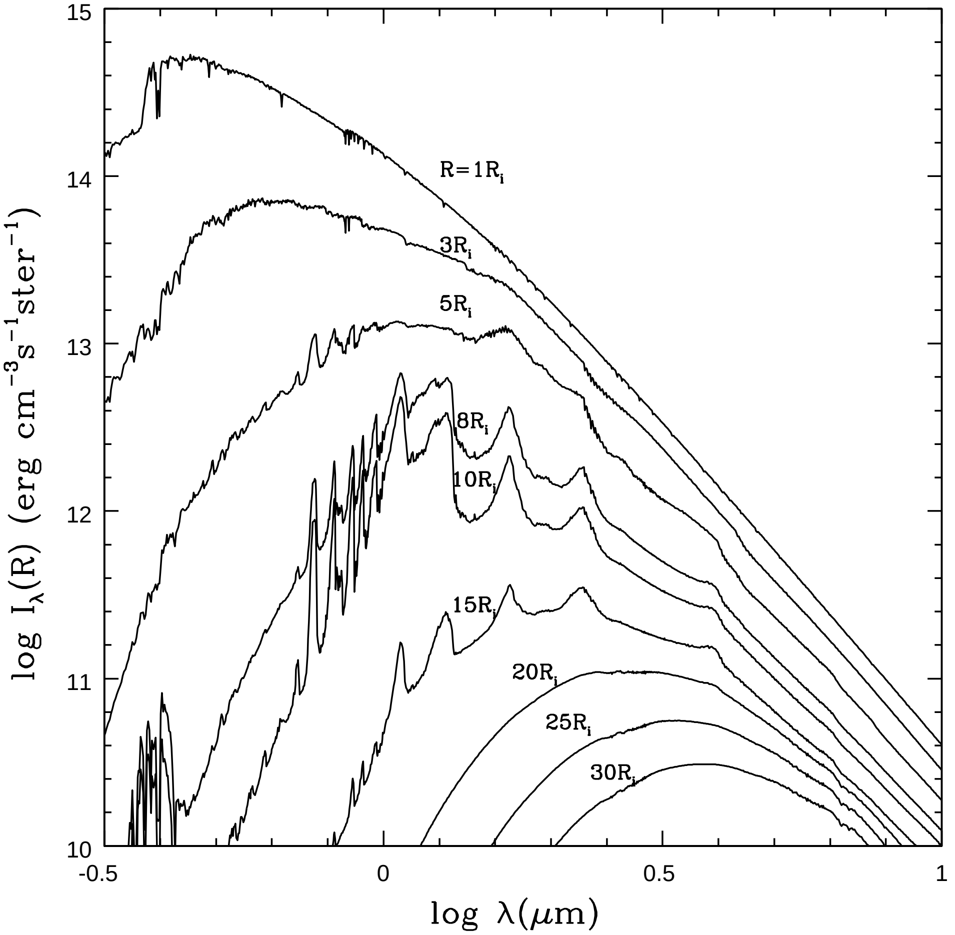

Fig. 4.— Emergent intensities from selected annuli of the disk model calculated for a 55 degree emergent angle. Effective temperatures of the annuli at 1, 3, 5, 6, 8, 10, 15, 20, 25, and 30 R$_i$ are 6420, 4660, 3400, 2480, 2130, 1630, 1310, 1110, and 977 K, respectively. Molecular absorption features in the near-IR arise from cool regions of the disk, which do not contribute to the optical spectrum.

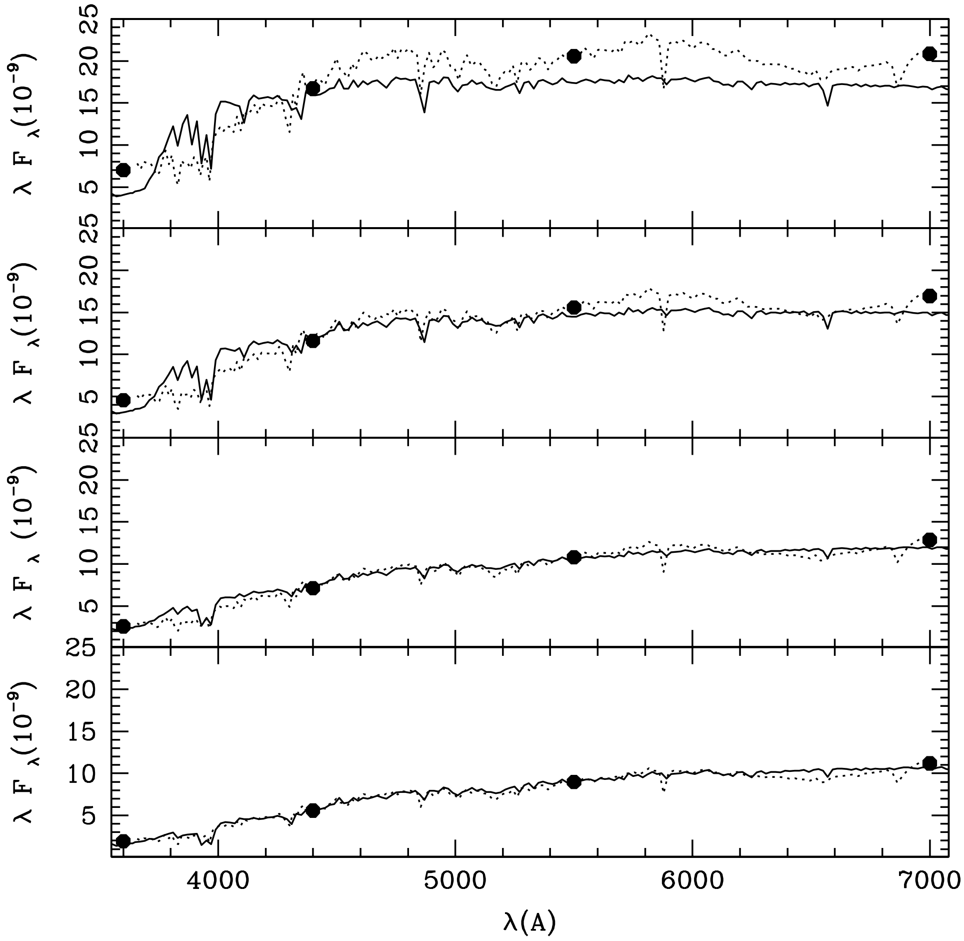

Fig. 5.— Observed UBVR photometry and optical spectra with different A$_V$: 2.2,1.9,1.5,1.3 (dotted lines, from top to bottom) and model spectra with T$_{max}$: 7240, 6770, 6420, 5840 (solid lines, from top to bottom). The total flux spectra are produced by weighting the intensities (Figure 4) by the appropriate annular surface areas.

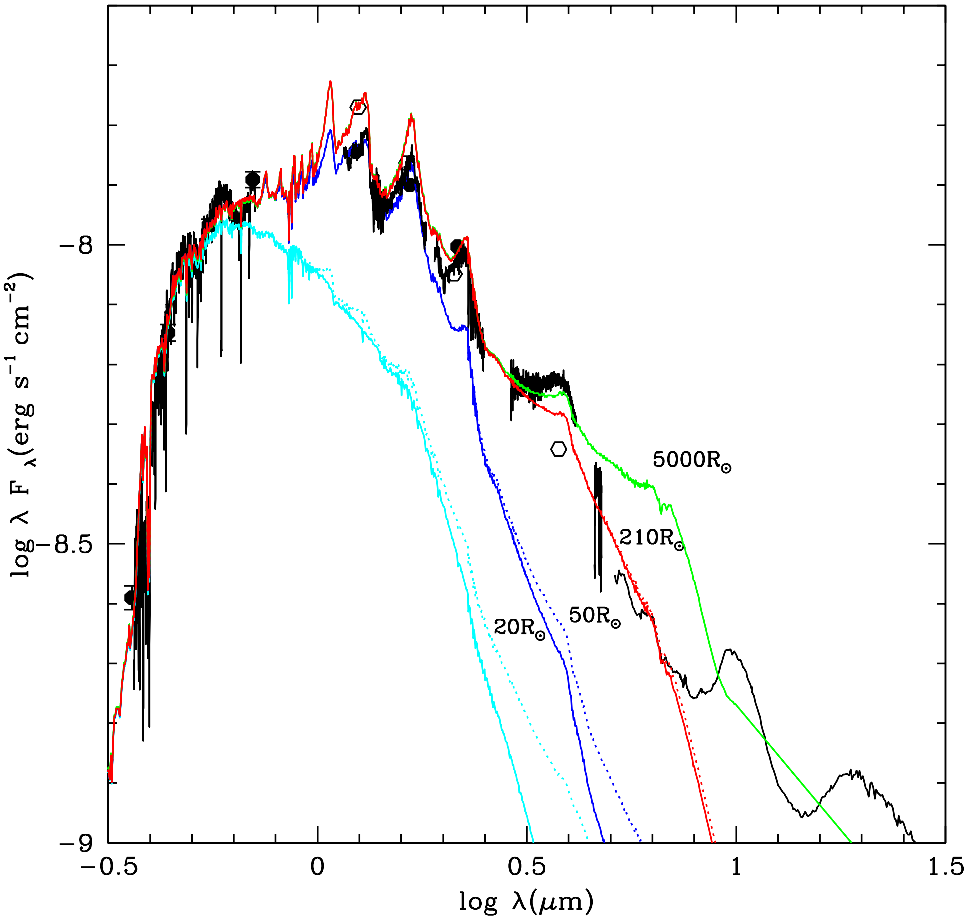

Fig. 6.— Comparison between observed data and disk models for different values of the outer radii. All the black lines and dots are observed spectra and photometry data as shown in figure 1. All the color lines are model spectra. The parameters of the disk models are inner disk radius 5 R$_\odot$, and $M\dot{M}\sim$ 7.2×10^{-5}M$_\odot$/yr. The corresponding T$_{max}$ is 6420 K. The four model spectra from top to bottom are for the disk models truncated at 5000 R$_\odot$, 210 R$_\odot$, 50 R$_\odot$ and 20 R$_\odot$. The solid lines are model spectra for a high mass accretion rate region with outer radii as shown. The dotted lines are spectra for models where an outer region with mass accretion one order of magnitude smaller has been added. For the disk model truncated at 5000 R$_\odot$, the dotted line is coincident with the solid line. The extinction parameter is A_V=1.5.

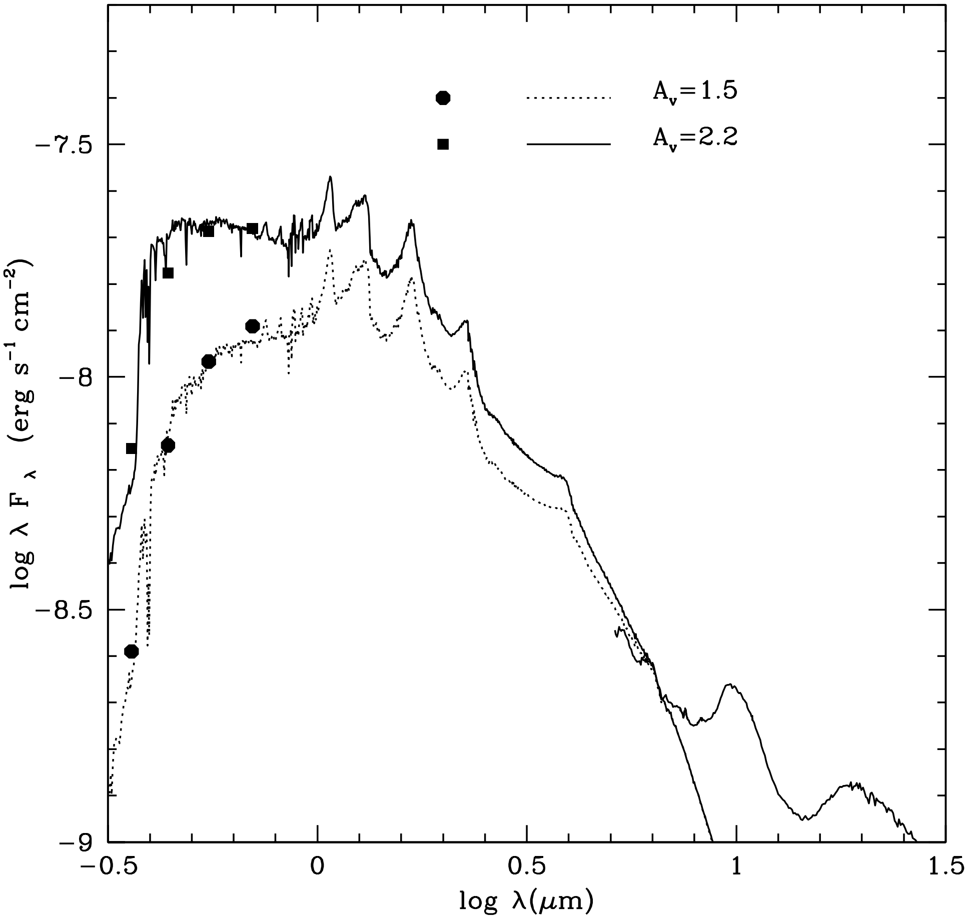

Fig. 7.— Two truncated models fitting the observations corrected by A_V=2.2 and A_V=1.5. Only optical photometries and IRS spectra (5-30 microns) are shown. The square points are the photometries corrected by A_V=2.2, while the round points are the photometries corrected by A_V=1.5. The IRS spectra corrected by these two A_V are coincident. The solid line is the model fitting to observations with A_V=2.2, while the dotted line is the model fitting to observations with A_V=1.5. Both of the two models have the same outer radius of the high state R_{out}=210 $R_\odot$.

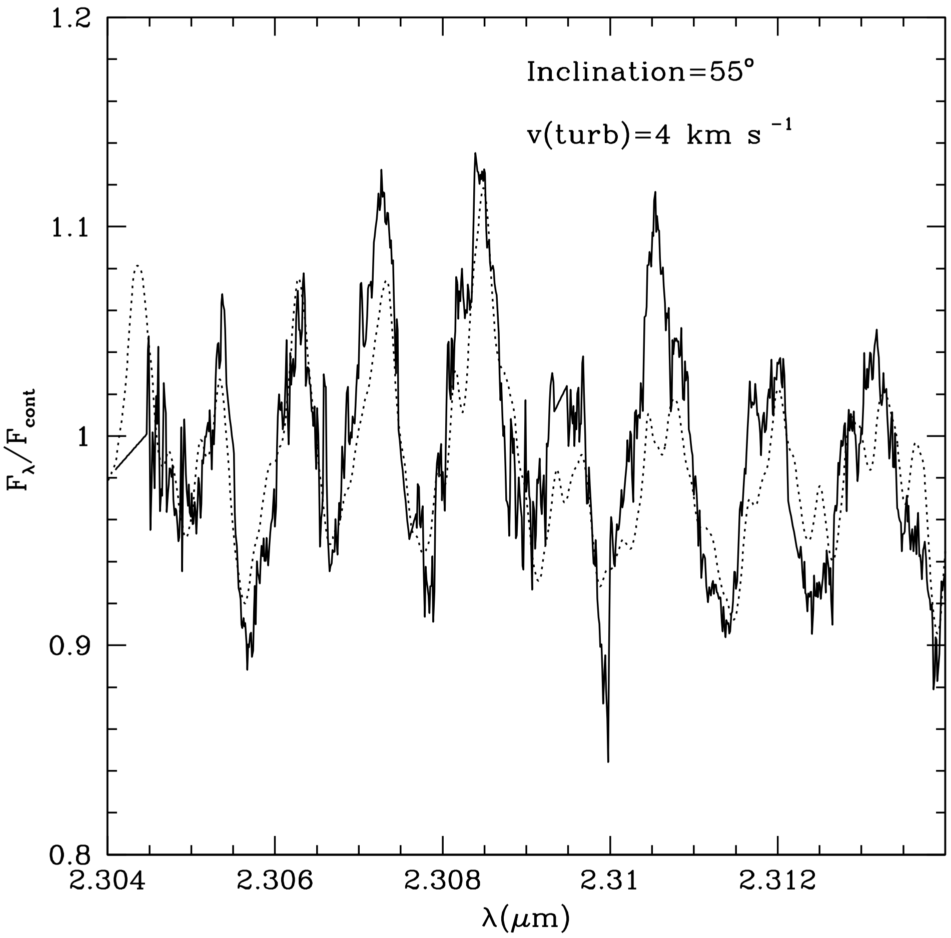

Fig. 8.— CO first overtone absorption band around 2.3 μm. The solid line is the observed CO first overtone absorption feature from Hartmann et al. (2004) and the dotted line is the model spectrum after being convolved to the same spectrum resolution. The turbulent velocity is 4 $\mathrm{km\,s^{-1}}$ and the inclination angle is 55 degrees.

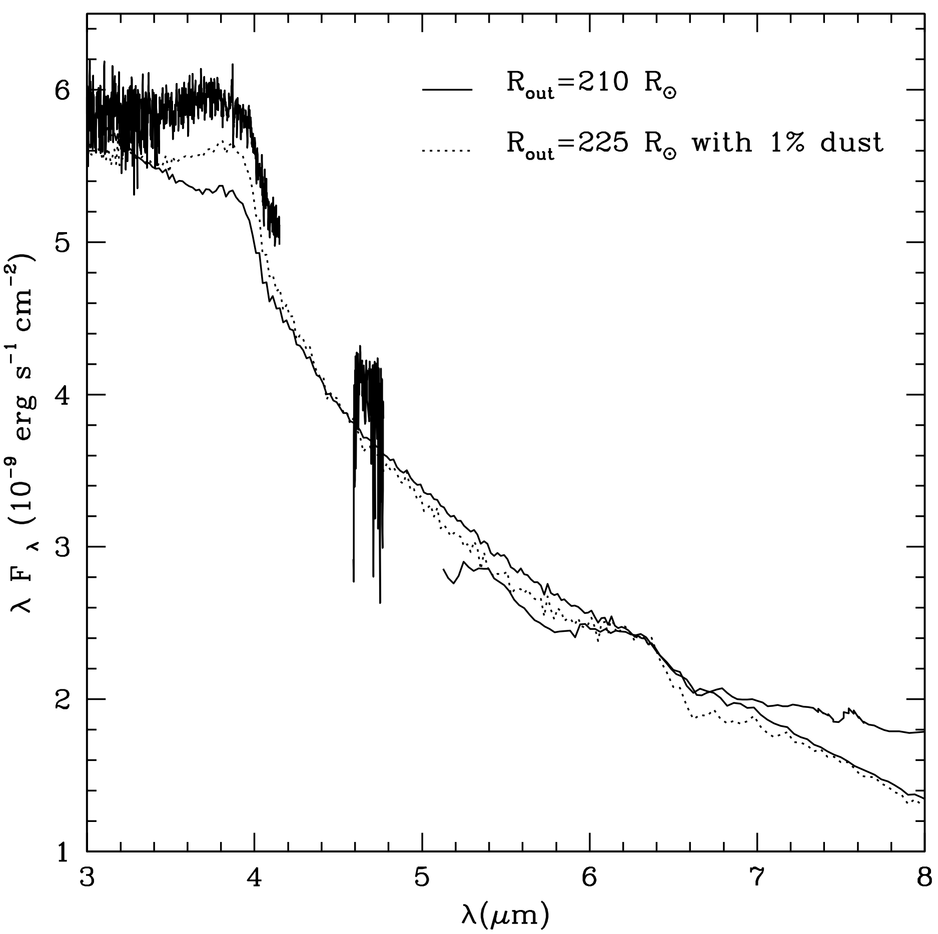

Fig. 9.— The mid-infrared part of the observed spectra in Figure 1 compared with the model spectra. The solid line is the model with R_{out}=210 $R_\odot$ and the dotted line is the model with 1 % dust opacity (dust opacity reduced by a factor of 100) and R_{out}=225 $R_\odot$. We do not have the CO fundamental opacities in our model and thus cannot reproduce these strong spectral features at 4.6 μm.

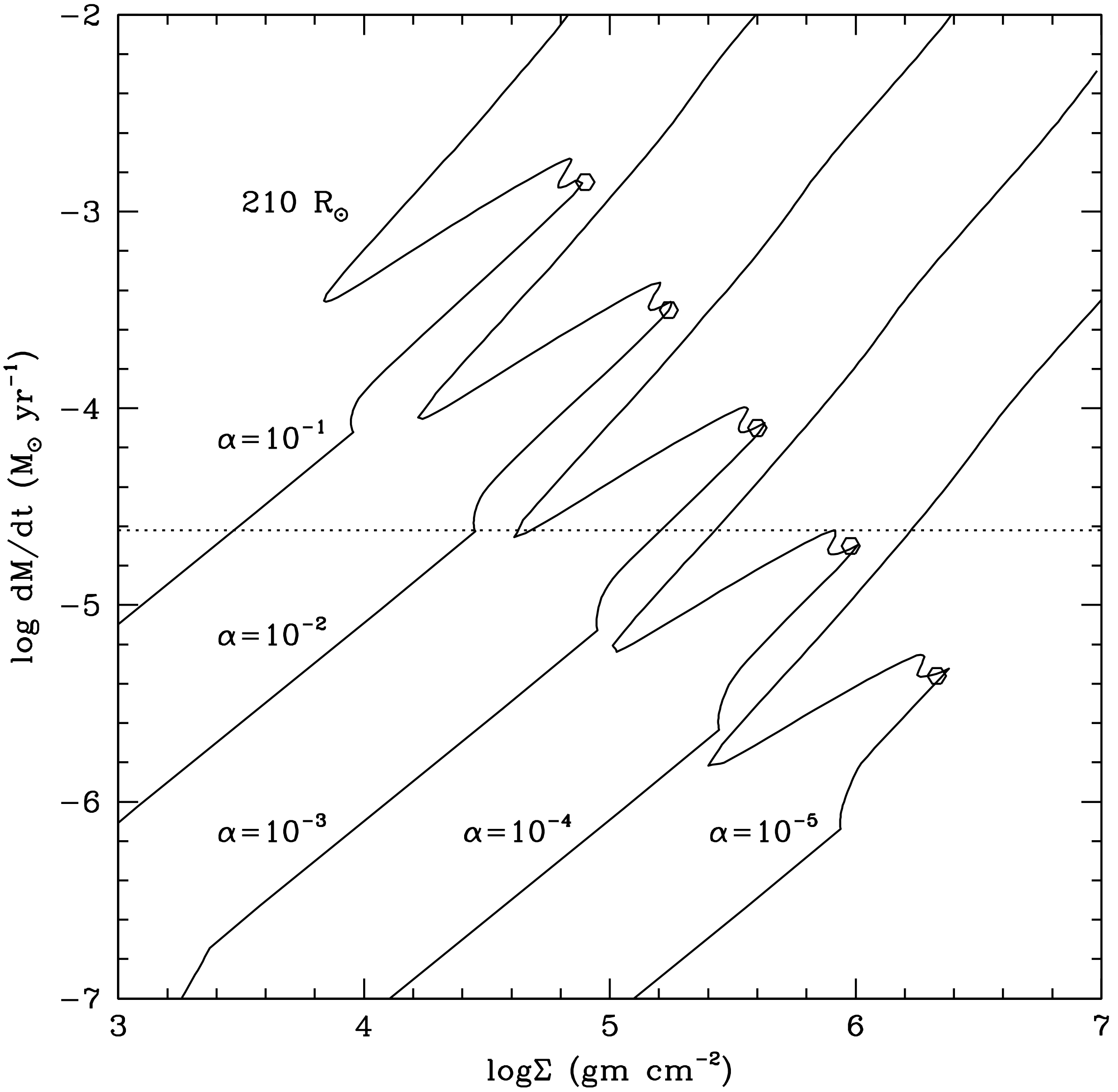

Fig. 10.— The equilibrium curves for thermal-instability at R=210 R$_\odot$ with five values of α: 10^{-1},10^{-2},10^{-3},10^{-4},10^{-5}(from top to bottom). The dotted line is $\dot{M} = 2.4 \times 10^{-5} M_\odot/yr$, set to be one order of magnitude lower accretion rate than the accretion rate of the inner disk. If the outer disk $\dot{M}$ were one order of magnitude higher than this (so that the outer disk and inner disk accretion rates are the same) the mid-infrared flux would be much larger than observed (see discussion in §4). The open circles denote the critical surface densities Σ_A for triggering the thermal instability at each value of α (see §5.3)